Chapter 6

Colloidosomes as Implantable Beads for the *in vivo* Delivery of Hydrophobic Drugs

Abstract. In this study we describe the synthesis of silica based colloidosomes with a polymer core obtained via inverse Pickering emulsification and their use as an implantable drug delivery system in zebrafish. Silica nanoparticles act as a stabilizer of a water-in-oil emulsion creating aqueous droplets with a silica shell. The core of the colloidosomes was polymerized to prepare tough particles. The colloidosomes were loaded with model drugs and the release characteristics were investigated and showed to be dependent on the porosity of the silica nanoparticles. Studying the effect of drugs on zebrafish development and tail regeneration is a new and emerging tool in biomedical research. To study the *in vivo* delivery and bioactivity of a model drug, colloidosomes loaded with retinoic acid were implanted subcutaneously in partially amputated caudal fins and the biological effect of released retinoic acid on the fin regeneration was studied at the phenotype and genotype level. The biocompatibility of the colloidosomes was demonstrated as no signs of inflammation were observed. With these initial studies we demonstrate that colloidosomes can be used as a single implanted bead to locally release drugs *in vivo*. It is envisioned that these single particles can be applied for a broad range of hydrophobic drugs.

6.1 Introduction

Solid particles can strongly interact and undergo self-assembly onto the liquid/liquid or liquid/gas interface allowing the formation of Pickering emulsions.[1] During the last decades this type of emulsification attracted extensive attention due to their strong stability compared with their surfactant-stabilized analogues.[2] The emulsion droplets serve as a template for the assembly process of solid nanoparticles, leading to numerous potential applications.[3-5] The particle assembly at the water-oil interface can be stabilized using different strategies including electrostatic binding with polyelectrolytes,[5] van der Waals forces,[6] sintering,[7] gelation,[8, 9] chemical cross-linking[10, 11] and inter-particles polymerization.[10] Due to the structural analogy of these microcapsules with liposomes, they are often called colloidosomes.[6] These assemblies were intensively studied by Velev and collaborators[5], and the driving force of the colloidosomes formation is the decrease of energy at the liquid/liquid interface. Several properties can be tuned by design including wall thickness, porosity and chemical composition.[2] Because colloidosomes are surfactant-free assemblies, any toxicity issues related to surfactant molecules is absent.[12] Therefore these particles are attractive for many potential applications such as food technology and the delivery of poor water soluble compounds.

Colloidosomes were studied as a potential drug delivery system, but so far only *in vitro* studies have been investigated. Prestidge studied the release profiles of dibutylphtalate, a lipophilic model compound, from colloidosomes stabilized by Aerosil™.[13] A polydimethylsiloxane-in-water emulsion stabilized with silica nanoparticles was used and the drug release profile was investigated and showed to be dependent on the colloidosome shell composition. Zhang and coworkers[14] studied the synthesis of empty core microcapsules with a hybrid shell composed of two layers: non-porous silica nanoparticles and a polymer layer. It was shown that the release kinetics of a methylene blue chosen as model drug was influenced by the wall thickness of the microcapsule. Destribats *et al.*[15] designed colloidosomes stabilized by Aerosil™ nanoparticles with a wax core. Upon heating the core expands thereby cracking the outer shell, leading to the release of the liquified core. Although Pickering stabilized emulsions were extensively studied and several investigations on drug release were described, actual *in vivo* studies of these microcapsules are still a pristine area of research.

The versatile nature of colloidosomes synthesis makes these microparticles a good candidate to design a potential drug delivery system. Depending on the viscosity of the

phases used for the emulsion, and the size and shape of the nanoparticles, it is possible to prepare colloidosomes with a sized diameter ranging from few hundred nanometers to the submillimeter length scale. In this chapter we used 100 μm colloidosomes, stabilized with silica nanoparticles (200 nm) and with a polyacrylamide core. The obtained microcapsules are tough materials and can be manipulated with a tweezer. Thus single colloidosomes were used as a local implant for the *in vivo* delivery of a drug in specific area in the tail of the zebrafish as a model system of rheumatoid arthritis (RA).

RA is an immune-mediated inflammatory disease and it is characterized by a chronic inflammation of the joint tissue resulting in a degeneration of joint structures. [16,17] Although the causes of RA are still unknown, it has been established that all-*trans* retinoic acid (ATRA) plays a pivotal role in the reduction of the inflammation.[18] Several experiments with collagen-induced arthritis (CIA) rodents showed that retinoids significantly decrease the course of the symptoms in RA. Moreover, Kirchmeyer and collaborators[16] have found that ATRA inhibits the inflammatory process in the joint tissue of CIA rats. Nozaki *et al.*[19] confirmed that ATRA reduces the amount of inflammatory signals in murine CIA, suggesting that this molecule might also be effective for the treatment of inflammatory arthritis as human RA. ATRA is a versatile compound which may be used for the treatment of several diseases including different type of cancers.[20, 21] However the concentration in the living organisms must be in a precise range.[22] Side effects generated by ATRA are common and severe and include liver toxicity, renal failure and it has a teratogen effect in embryos.[22] Studying the pharmacological effects of new drugs have traditionally been performed in mammals. However since the nineties the zebrafish (*Danio rerio*) is becoming an important and versatile tool for drug screening and discovery studies.[23, 24] Zebrafish embryos are widely used for genetic investigations as the 75% of the *Danio rerio* genome is in common with the human genome. Furthermore their external development and their optical transparency allow the detection of any morphological deformations as a consequence of the effects of an admitted drugs.[25] This animal model is also exploited in its adult stage due its ability of caudal fin regeneration after surgical amputation.[26] During the development of new part of the fins there are several cellular signals involved in the process very similar to some of those that affect bone and cartilage differentiation in mammals and humans.[27] Géraudie and collaborators[28] have shown that ATRA delays the caudal fin regeneration proving that adult zebrafish is a suitable model for skeletal diseases in humans.[27]

However, the hydrophobic nature of ATRA makes the delivery of this compound challenging. Administered ATRA must be effective in restricted area of the joint and the blood circulation must be minimized to lower side effects. Therefore the design of a local release delivery system compatible with zebrafish assays is needed. In this study, we investigated single colloidosomes as a new tool for the local ATRA delivery in partially amputated adult zebrafish caudal fins and the effect on the regeneration was studied.

6.2 Results and discussion

6.2.1 Colloidosomes synthesis and characterization

Colloidosomes were synthesized following the general scheme outlined in **Figure 1**. In our approach the water-in-oil emulsion is stabilized by silica nanoparticles and the core is composed of cross-linked hydrogel.

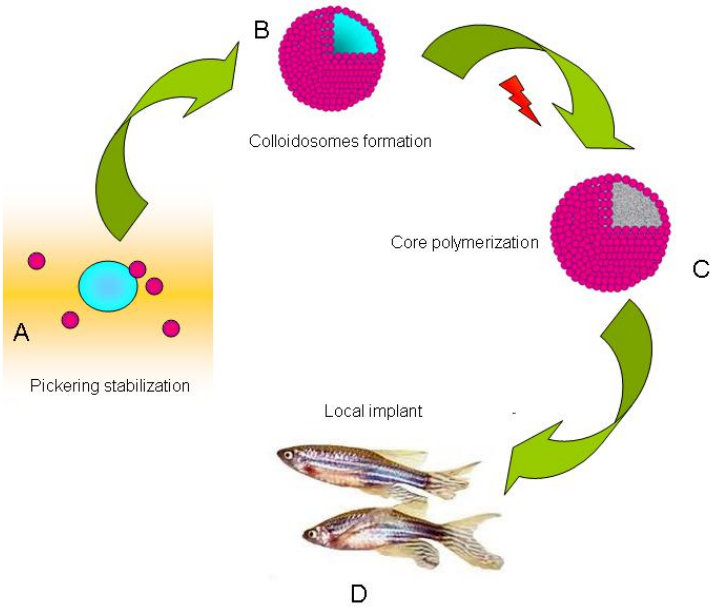

Figure 1. Schematic illustration of the silica stabilized colloidosomes with polymeric core. (A and B) Silica nanoparticles are dispersed in the oil phase. The suspension is mixed with the water phase containing the monomers resulting in a stable emulsion. (C) The Pickering colloidosomes are further stabilized by polymerization of the particle core. (D) The microcapsules were subsequently implanted in the amputated portion of adult zebrafish caudal fin.

In this chapter three types of silica nanoparticles (SNPs) were used mesoporous silica nanoparticles (MSNs), co-condensed functionalized mesoporous silica nanoparticles and non-porous silica nanoparticles. Mesoporous silica nanoparticles (MSNs) were synthesized *via* the sol-gel technique using hexadecyltrimethylammonium bromide (CTAB) as a template and tetraethylethoxysilane (TEOS) as organic precursor. The resulting

nanoparticles were composed of parallel channels throughout the particles as confirmed by transmission electron microscopy (as hown in **Chapter 2**, **Figure 2B**). A uniformity in size and shape of the synthesized particles with a diameter of approximately 200 nm was observed with scanning electron microscopy (SEM) as shown in **Figure 2A**. The used surfactant CTAB is known to be toxic and therefore the removal of this compound from the nanoparticles is critical for *in vivo* drug delivery studies. [29] The nanoparticles were refluxed overnight in acidic methanol and the removal of the surfactant was confirmed by Fourier transformed infra-red spectroscopy (FT-IR) analysis (as shown in **Chapter 2**, **Figure 1**).

Next, co-condensed MSNs were synthesized accordingly to a procedure of Trewyn and collaborators.[30] In this method the synthesis occurs in the presence of CTAB as a template using a mixture of TEOS and 3-mercaptopropyltriethoxysilane. This results in the introduction of functional groups on the surface and in the channels of the mesoporous nanoparticles. SEM analysis revealed that the resulting particles were homogenous in size with an average diameter of 200 nm (**Figure 2C**). Afterwards the template was removed and the thiol groups were converted with 2,2'-dithiopyrydine to disulfide-2-dithiopyrydine groups.

Non-porous silica nanoparticles were synthesized using the Stöber method.[31] The particles were homogenous in size and shape as confirmed by scanning electron microscopy with an average diameter of approximately 190 nm (**Figure 2B**). The absence of a template during the synthesis leads to the formation of spherical non-porous nanoparticles.

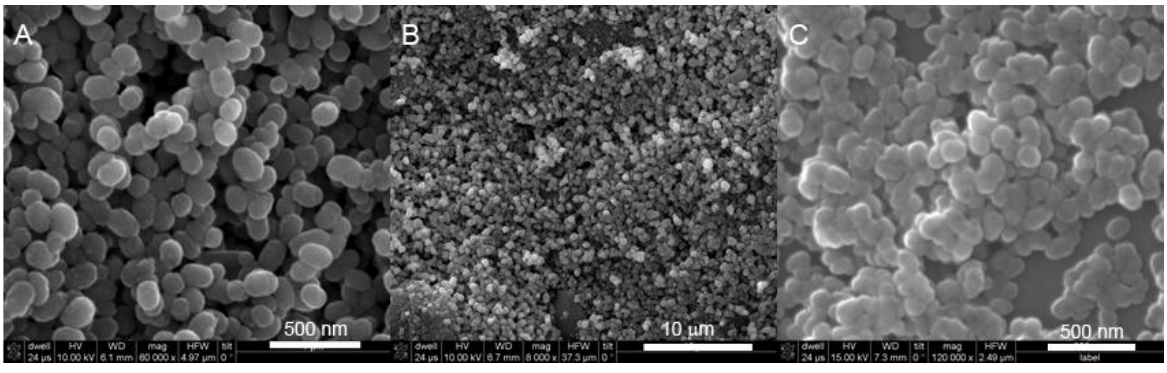

Figure 2. Scanning electron microscopy (SEM) images of the silica nanoparticles. Silica nanoparticles synthesized with the template technique (A), using the co-condensed method (B) and the Ströber method (C). All the nanoparticles are spherical and size uniformity was observed.

Subsequently the three different types of silica particles were used to stabilize the formed Pickering emulsion. Emulsions were prepared by dispersing the nanoparticles in sunflower oil and mixing this with an aqueous solution containing N-isopropylacrylamide and N,'N-

methylenediacrylamide under ultrasonic emulsification conditions. This resulted in stabilized droplets with an average of 100 μm. To investigate the release kinetics of small molecules from the colloidosomes the aqueous phase also contained in some cases rhodamine B. An aqueous solution of N,N,N'N',-tetramethylenediamine and ammonium persulfate were added to initiate the polymerization of the aqueous core. The microparticles were stirred for 30 minutes at room temperature and the colloidosomes were separated from the oil phase by centrifugation. Next, the microcapsules were rinsed with ethanol to remove excess of oil and stored at room temperature until further use. The colloidosomes were imaged with optical microscopy before polymerization in order to observe the shell structure composed of the silica nanoparticle (**Figure 3A)**. After polymerization of the acryl monomer (**Figure 3B1** and **3B2**) the microcapsules appear opaque and the nanoparticles shell was no longer visible. The emulsion contained stabilized droplets with an average diameter raging from 80 μm to 100 μm, which did not change upon polymerization. As shown in **Figure 3B3** the colloidosomes have homogenous size and shape.

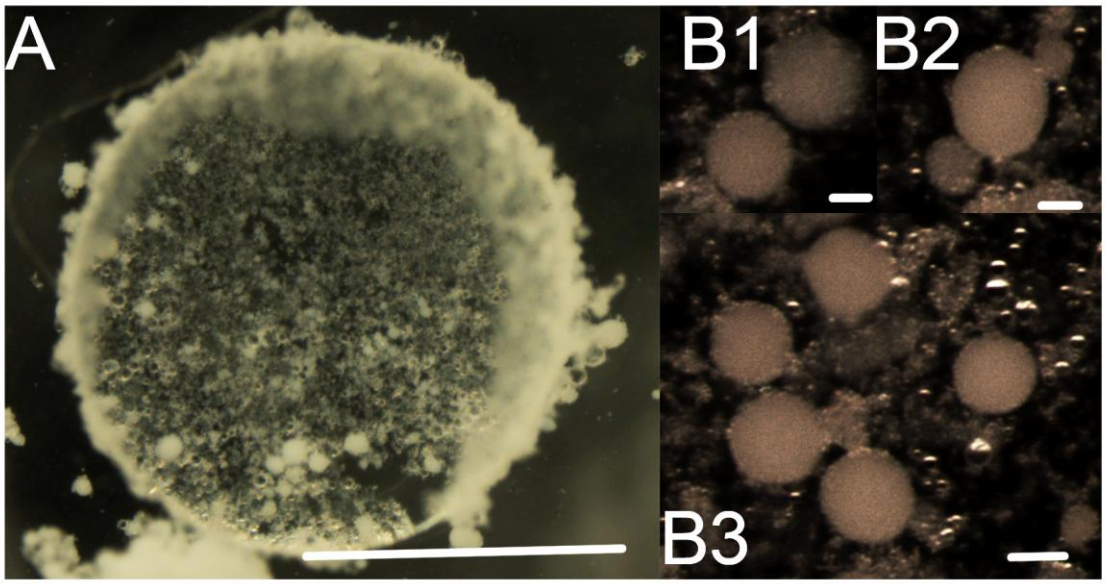

Figure 3. Bright field image of mesoporous silica nanoparticles stabilized collodoisomes.(A) An external shell of silica nanoparticles is observed enveloping the microdroplet of water in the dispersing oil phase. Before the core polymerization is possible to observe the nanoparticles structure. (B1 and B2) However, when the core polymerization is completed the microparticles are white and opaque as shown in the bottom right image. (B3) The stabilized colloidosomes show homogenous size and spherical shape. Scale bar 50 μm.

Scanning electron microscope (SEM) analysis of colloidosomes revealed that the microcapsules showed a narrow size distribution as confirmed by bright field microscopy and they had a spherical shape (**Figure 4**). In some cases the spherical shape of the polymerized colloidosomes was preserved under the high vacuum conditions of the electron microscope showing the toughness of the particles. This is an important parameter

for the *in vivo* experiments since single microcapsules were implanted using Dumont® tweezers in the caudal fin.

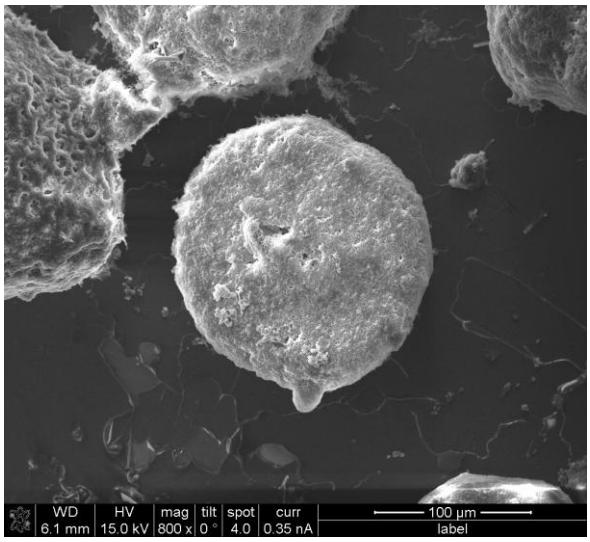

Figure 4. Scanning electron microscopy image of silica stabilized colloidosomes. Silica nanoparticles are observed forming a homogenous shell around the polymeric core. The microparticles have a spherical shape and maintain their original shape due to of the polymerized core.

6.2.2 Release kinetics study

The release kinetics of small molecules was investigated with UV-VIS spectroscopy using rhodamine B as a model compound. In order to evaluate whether the mesoporosity of the silica nanoparticles affects the kinetics, the release of rhodamine B from colloidosomes which were prepared with either mesoporous or non-porous silica nanoparticles was studied (**Figure 5**).

A significant difference in release kinetics was observed depending on the type of silica used. Colloidosomes with a shell composed of mesoporous nanoparticles released 50% of the fluorescent dye in approximately 1 hour. In contrast, the same amount of dye was only released in approximately 3 hours when the colloidosomes were stabilized with non-porous silica nanoparticles. This shows that the porosity of the external shell has a strong influence on the release profile indicating that the dye also diffuses through the mesoporous silica particles. Both the porous and non-porous nanoparticles used for the preparation of the colloidosomes have a similar average diameter and shape. Thus, the rate of dye release is influenced solely by the internal nanoparticle structure and not by the inter-particle spaces between the SNPs, which are equivalent in all the colloidosomes studied.

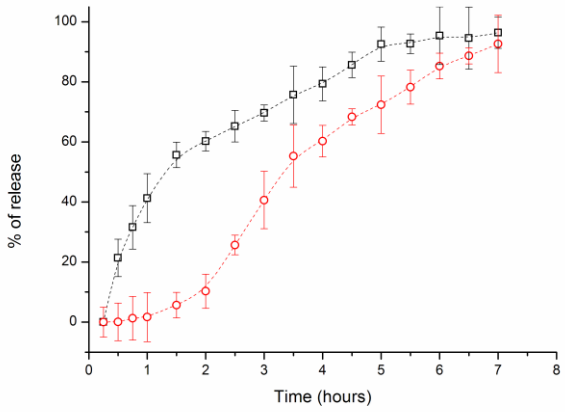

Figure 5. Release of fluorescent rhodamine B from 100 mg of silica-nanoparticle stabilized colloidosomes. Observed release for mesoporous silica nanoparticles stabilized colloidosomes (□) and non-porous silica nanoparticles colloidosomes (○). The shell composition influences the rhodamine B release rate.

The mesoporosity of the external silica nanoparticle layer is important as the internal channels can be functionalized independently[32] thereby controlling the release properties of the colloidosomes. Thus, this opens up the possibility to covalently bind a drug on the outer MSNs layer while in the colloidosome core a different compound is encapsulated. Alternatively functionalized pores can be used to block the pores by steric hindrance resulting in a delayed release of the content from the core. This modified layer of MSNs acts in a similar way to non-porous stabilized colloidosomes.

Co-condensed mesoporous nanoparticles presenting free thiol groups on the surface of the pores were synthesized and modified with 2,2'-dithiopyridine moieties whose release can be detected via UV-VIS spectroscopy. Addition of dithiothreitol (DTT) resulted in the reduction of the disulfide bond and the release of 2-thiopyridine. The release of rhodamine B from the colloidosome core was also measured at the same time. A burst the release of 2-thiopyridine was observed while the rhodamine B is retained in the core showing a significant lag-time. When the thiopyridine is hydrolyzed completely from the mesopores of the silica shell the rhodamine B was released significantly in the supernatant. In future experiments, actual drugs bearing a thiol group, will be used.

This experiment showed the importance of the external mosoporosity of the silica shell on the release properties of the colloidosomes. If the pores are blocked with thiopyridine groups, the release of rhodamine B from the core is similar to the release from non-porous silica stabilized colloidosomes (compare **Figure 5** and **6**).

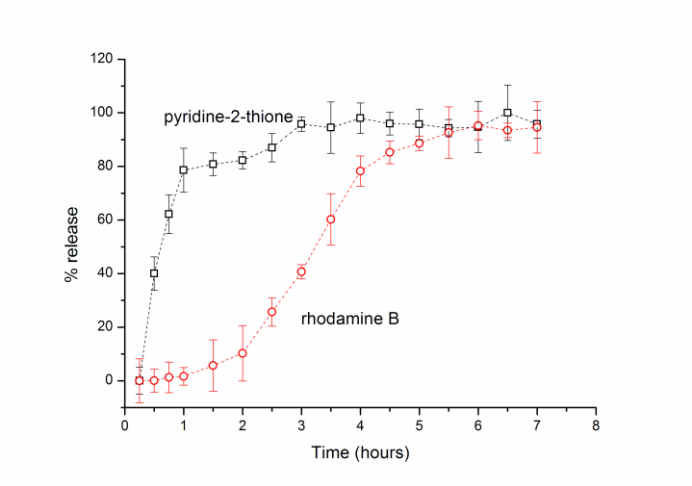

Figure 6. Release of rhodamine B and pyridine-2-thione from 2-pyrdylthio-modified mesoporous silica nanoparticles after the addition of DTT. A burst release of the shell-encapsulated pyridine-2-thione is observed, while the core-encapsulated rhodamine B shows a significant lag time as the release is hindered by the presence of unreduced 2-pyridylthio in the channels of the mesoporous silica nanoparticles.

6.2.3 *In vivo* investigations of Pickering stabilized colloidosomes

In order to study the potential *in vivo* application of these microcapsules we used them as a local delivery system in adult *Danio rerio*. Zebrafish caudal tail naturally regenerates when amputated. However, this process is delayed in the presence of *all-trans* retinoic acid (ATRA).[26] To study the regeneration process we amputated the ventral portion of the caudal fin. First, the regeneration in absence of silica stabilized colloidosomes was investigated and the rate of regrowth of the caudal fin was comparable with previous works.[26, 28] Control colloidosomes were stained with methylene blue for visualization during the surgery. A single microcapsule was implanted in the ventral portion of the caudal fin with a sterile tungsten needle in an incision before the first fin bifurcation. Next, the remaining part of the fin was amputated as shown in **Figure 7** and **Figure 8**.

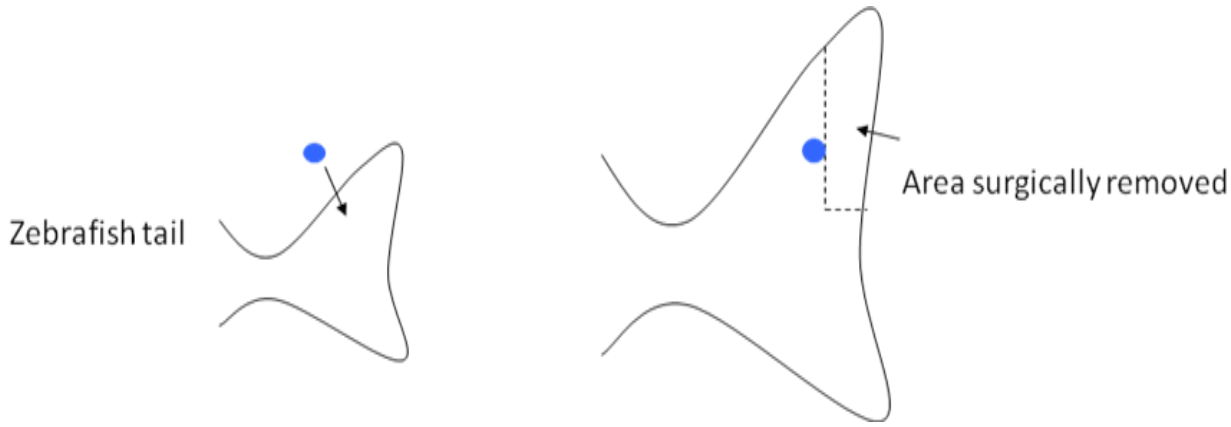

Figure 7. Schematic representation of Zebrafish surgery for microcapsules implantation. Zebrafish were anesthetized using MS-222 and placed between two layers of wet paper. A wound was made with sterile tungsten needle and a microcapsule was implanted in the cut. Next, the

dashed area was removed with a sterile scalpel to avoid infections. The animal was then put in fresh water to recover.

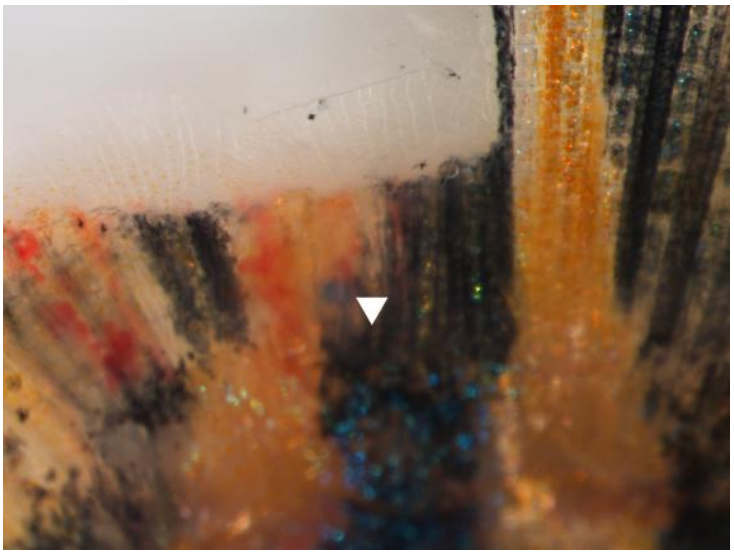

Figure 8. Bright field optical image of operated Zebrafish tail. The implanted microcapsule is highlighted with the white arrow and it was stained with methylene blue for visualization.

The newly forming tail was similar to the control experiment as no malformations were observed, (**Figure 9A** and **C**). Next, a single retinoic acid-loaded colloidosome was implanted in the caudal fin of adult zebrafish. For this study colloidosomes with a non-porous silica nanoparticle shell were used due to their delayed release of a drug. Thus enough time was given to perform the surgery on the zebrafish and to implant a single microcapsule without premature release. The microcapsules used were loaded overnight with 10 mg/mL of ATRA, and they were washed with PBS before surgery.

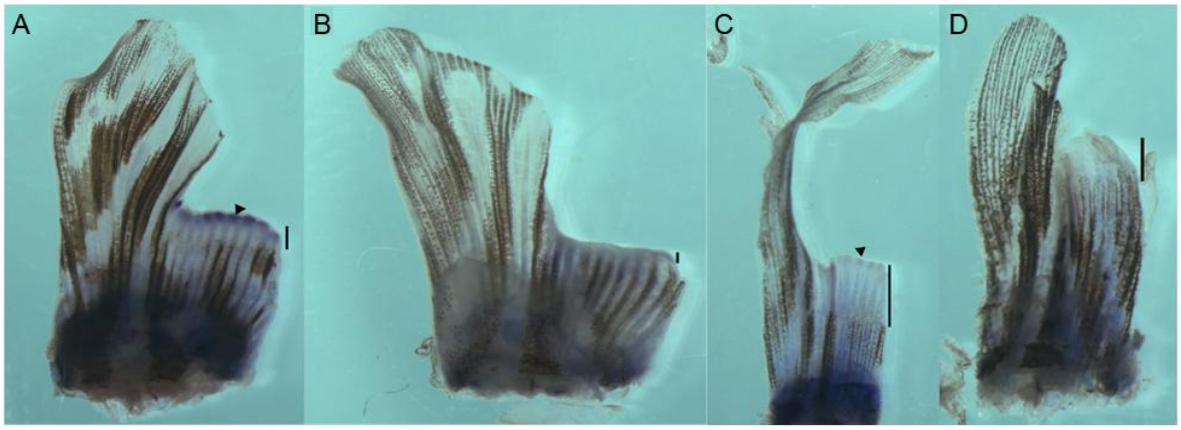

Figure 9. Bright field images of partially amputated adult zebrafish caudal tails. (A and C) Control samples bearing an implanted empty microcapsule and imaged after 2 and 9 days respectively. (B and D) Zebrafish caudal fins after implantation of an ATRA loaded microcapsule and imaged after 2 and 9 days respectively. A delay in regeneration is observed when ATRA is released from the implanted microcapsule in the tail. In A and C is shown the expression of *msxB* gene (blue) at the edge of newly formed tissue, as shown by the black arrow. Differences in regenerated caudal tail are highlighted with black segments placed next to the tail.

One hundred male adult zebrafish were used in the experiment: fifty fish received a control microcapsule while in fifty zebrafish an ATRA-loaded colloidosome was implanted. Every 2 days 10 control zebrafish of both groups were euthanized and analyzed, this procedure was done up to 10 days. All control zebrafish were found healthy at all time intervals and the caudal fin showed regenerated tissues as reported in literature.[26] The zebrafish implanted with ATRA-loaded colloidosomes were also found in healthy conditions, however a clear delay in tail regeneration was observed due to the released ATRA.

Tail regeneration in zebrafish is activated by a number of specific genes. The *msxB* gene was selected to study the effect of ATRA on the regeneration of the caudal fin.[26] The activation of this gene was investigated with a standard *in situ* hybridization technique. In **Figure 9A** and **C,** the regenerated portion of the control tail presents a strong and clear expression of the *msxB* gene at the edge of the new tissue visualized by the purple color at the edge of regenerated tail. In treated zebrafish (**Fig. 9B** and **D**) the regenerated part of the tail showed a lower expression of the *msxB* gene as a result of released ATRA from the implanted colloidosome.

The length of the regenerated tissue was measured as a function of time and a difference in the rate of regeneration was observed (**Fig. 10**). When empty microcapsules were implanted the caudal fin regenerated completely to the natural pre-amputated length (white bars). However, a significant delay was observed in the presence of ATRA loaded implanted microcapsules. Thus, this result shows that ATRA is released from the colloidosome in its bioactive form and an evident interaction with the biological pathways of the regeneration process is observed.

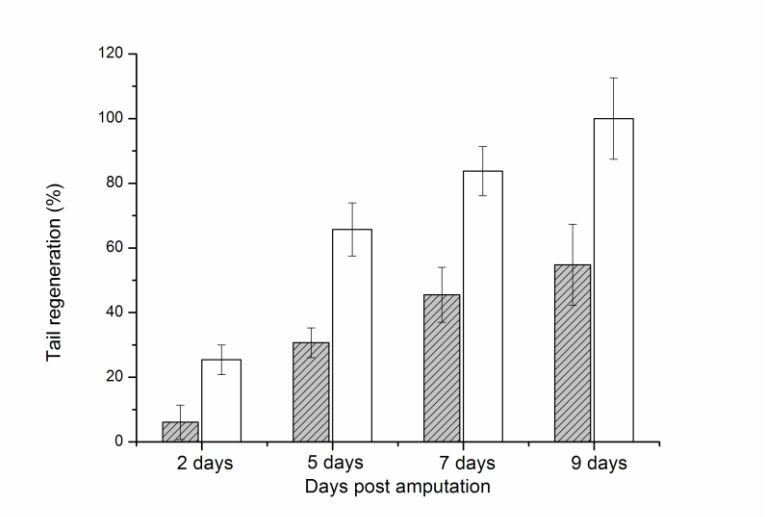

Figure 10. Caudal fin regeneration of amputated tails. The white bars refer to the control animals implanted with ATRA unloaded microcapsules. The gray bars indicate the regenerated tissue of

caudal fins after implantation of ATRA loaded microcapsules. The regenerated tissue was measured with Leica software of a stereo fluorescence microscope M16ZF.

6.3 Conclusions

This study is one of the first example in which Pickering stabilized colloidosomes are used as an *in vivo* drug delivery system in zebrafish. Colloidosomes formed from an inverse Pickering emulsion stabilized with silica nanoparticles and polymer core were synthesized. The release properties of small molecules showed to be depending on the silica nanoparticles used for the outer shell. A direct dependence between shell composition and drug delivery was observed. A potential application of co-condensed nanoparticles stabilized colloidosomes is the delivery of multiple drugs with different release rates. However further research is needed to study the potential of this double drug delivery system in which actual drugs will be studied. We tested our microcapsules with non-porous nanoparticles shell as an implant *in vivo* in adult Zebrafish for the local delivery of ATRA. This caused a delay in caudal fin regeneration as observed by the morphological and gene analysis. This study showed the biocompatibility of the colloidosomes as no malformations or inflammations were observed in treated fish. The heterogeneous structure of the colloidosomes opens up possibility to delivery hydrophilic compounds from the core while hydrophobic compounds may be delivered from the mesoporous silica nanoparticles shell. Moreover, the external shell controls the release profile of the cargo, and the role of a double container in with a different drug can be hold in the nanopores towards selective functionalization. Due to the versatility of these microcapsules we envision that further studies are necessary to investigate potential application of these colloidosomes as drug delivery system in animal models.

6.4 Experimental part

Materials. Acetic anhydride, alkaline phosphatase (AP), alcian blue, ammonium persulfate, bovine serum albumin (BSA), 3-[(3-cholamidopropyl)-dimethylammonio]-1-propanesulfonate (CHAPS), 2,2'-dithiopyrydine, ethylenediaminetetracetic acid (EDTA), ficol 400, formamid, heparin, hexadecyltrimethylammonium bromide (CTAB), yeast RNA, magnesium chloride ($MgCl_2$), methyl salicylate, N-isopropylacrylamide, N,'N-methylenediacrylamide, N,N,N'N',-tetramethylenediamine, paraformaldehyde (pFA), potassium chloride (KCl), *all-trans* retinoic acid (ATRA), 2-propanol, sodium chloride (NaCl), sodium hydrogen phosphate (Na_2HPO_4), sodium hydroxide, triethanolamine (TEA), tetraethyl orthosilicate (TEOS), trichloroacetic acid (TCA), tris(hydroxymethyl)aminomethane HCl (TRIS-HCl), Tween 20, hydrochloric acid (HCl) and retinoic acid (RA) were purchased from Sigma Aldrich and used as received.

Milli-Q water with a resistance of more than 18.2 MΩ/cm was provided by a Millipore Milli-Q filtering system with filtration through a 0.22 μm Millipak filter. 2-[Methoxy(polyethyleneoxy)propyl]trimethoxysilane was purchased from ABCR GmbH & Co. KG, while all the reagents for *in situ* hybridization (ISH) have been purchased from Roche Diagnostics. Phosphate buffer saline (PBS) was composed of 2.74 M of NaCl, 54.0 mM of KCl, 210 mM of $Na_2HPO_4*2H_2O$ and 30.0 mM of KH_2PO_4 and this solution was diluted 20 times to reach the final concentration. The solution of PBS-Tween (PBS-T) was composed of PBS containing 0.1 % of Tween 20. Zebrafish samples were analyzed after the surgery with a Leica MZ12 with DC500 camera equipped and a Zeiss Axioplan Imaging 2 with MRc5 camera. UV-VIS absorbance spectra were measured with a PerkinElmer Lambda 25 UV-VIS spectrometer.

Preparation of mesoporous silica nanoparticles. 2 g (5.48 mmol) of hexadecyltrimethylammonium bromide (CTAB) was dissolved in 960 mL of Milli-Q water with 7 mL of a solution 2N NaOH. The solution was heated at 80 °C for 30 min and 9 g (43.2 mmol) of TEOS was added. After 2 hours the suspension was filtered yielding a white solid powder (58% 5.22 g). The surfactant was removed from the particles by refluxing overnight in a mixture of methanol (310 mL) and fuming hydrochloric acid 12 N (31 mL) under an inert nitrogen atmosphere. After filtration a white powder with a yield of 60 % (5.13 g) was obtained. FT-IR analysis confirmed removal of the CTAB.

Preparation of non-porous silica nanoparticles. 2 g of tetraethoxysilane and 2.5 mL of an aqueous ammonia aqueous solution (25%) were dissolved in absolute ethanol (50 mL). The mixture was stirred at room temperature for 24 hours, and a white powder (yield 62%) was recovered via filtration.

Preparation of co-condensed mesoporous silica nanoparticles. 2 g of CTAB and 7 mL of a solution of NaOH 2N were added to 480 mL of MilliQ water and heated at 80 °C for 30 minutes. Subsequently a mixture of tetraethoxysilane (9 g, 43.2 mmol) and 3-mercaptopropyltriethoxysilane (100 mg, 0.42 mmol) were added and stirred at 80 °C for 2 hours. Next the surfactant template was removed with acidic methanol extraction as mentioned before. Nanoparticles (100 mg) were suspended in 10 mL of dimethylformamide and 2,2'-dithiopyrydine (100 mg, 0.045 mmol) was added. The suspension was stirred overnight and the particles were recovered by filtration resulting in a pale yellow powder. 100 mg of modified nanoparticles were collected and the reaction was considered quantitative.

Preparation of silica colloidosomes. 150 mg of silica nanoparticles previously synthesized were dispersed in 10 mL of sunflower oil and sonicated for 30 minutes in order to obtain a uniform suspension. In a separate container N,'N-methylenediacrylamide (70 mg, 0.45 mmol) and N-isopropylacrylamide (140 mg, 1.23 mmol) were dissolved in 2 mL of Milli-Q water. This solution was added to the oil phase with vigorous stirring until an inverse Pickering emulsion was formed. The polymerization of the core N,N,N'N',-tetramethylenediamine (100 μL, 0.67 mmol) was initiated by the addition of ammonium persulfate (10 mg, 0.05 mmol). The emulsion was continuously stirred for 30 minutes until the polymerization of the core was completed. The microparticles were collected by centrifugation and rinsed with ethanol (3x5 mL).

Electron microscopy analysis. The shape and size of the particles was characterized with scanning electron microscopy (SEM) using a NovaSem microscope. Samples were dispersed in 2-propanol, and 100 μL of this suspension was placed on an aluminum stub and dried at 37 °C under vacuum for 30 minutes. The samples were coated twice with a layer of carbon and imaged using an acceleration voltage of 15 kV. Transmission electron microscopy (TEM) was conducted on a JEOL 1010 instrument with an accelerating

voltage of 60 kV. Samples for TEM were prepared by placing a drop of each MSNs solution on carbon-coated copper grids. After approximately 10 minutes the droplet was removed from the edge of the grid with a tissue paper.

Dye release test. 100 mg of microcapsules were suspended in phosphate buffer saline solution (PBS, pH=7.24) containing 1 mM of rodhamine B and stirred overnight at room temperature. The suspension was rinsed 3 times with PBS in order to remove excess of rhodamine B. The samples were resuspended in PBS buffer and the release of the dye was measured in the supernatant with UV/VIS spectroscopy (542.75 nm, $\varepsilon = 1.06*10^6\ M^{-1}cm^{-1}$).

Preparation of microcapsules for zebrafish implantation. The microcapsules (100 mg) were loaded overnight with a 10 mg/mL of ATRA in DMSO and before implantation washed with PBS (3x2 mL). Control microcapsules were stained overnight with a 10 mM solution of methylene blue and washed with phosphate buffer solution (PBS) before implantation.

***In vivo* studies.** One hundred male *Danio rerio* (zebrafish) were bought in a local animal shop of Leiden, The Netherlands. The zebrafish were divided in 10 groups with 10 animals each group and placed in 10 separate tanks located in the aquarium facility of Leiden University. The temperature of the water was set at 25 °C and the temperature of the room was 23 °C. The animals were housed according to the European law (86/609/EC) and the Dutch government (Article 9). They were fed twice a day with commercially available dry fish food, and they had a dark/light cycle of 12 hours. Before surgery a solution containing 16 ppm of tricaine methane sulphonate (MS-222) was prepared in Milli-Q water and used directly to anesthetize the animals. A partial amputation of the caudal tail was operated and the bead was implanted between two fin rays as reported in the SI. The animals were placed in fresh water to recover and were monitored each hour for one day. For microscopy analysis the zebrafish were anesthetized. However, for further analysis the animals were then euthanized using a solution containing 90 ppm of MS-222.

***In situ* Hybridization (ISH).** For ISH analysis the msxB probe was used. The antisense RNA probes labelled with digoxigenin (DIG) were synthesized according to Bardine and collaborators.[33] After rehydration the tails were treated with proteinase K (0.5 µg/mL in PBS-Tween) for 8 minutes at room temperature, followed by enzyme inactivation with a solution of TEA 0.1 M and acetic anhydride 0.5 µL/mL in PBS-T for 10 minutes. The sample were washed 3 times with PBS-T and fixated in pFA 4% in PBS. The basic solution used for prehybridization and hybridization contained 50% deionized formamide, saline citrate, Denhart's, 1% of Tween-20, 0.1% of CHAPS (Sigma-Aldrich), 50 mg/mL of yeast tRNA (Sigma Aldrich) and EDTA. The Denhart's solution was prepared according to the procedure published by Jansen and collaborators.[34] The samples were prehybridized in this solution for 5 hours at 65 °C, followed by an overnight hybridization at the same temperature with the hybridization buffer containing the DIG labelled probe. Then the samples were washed with sodium chloride sodium citrate (SSC) buffer for six times and then with maleic acid sodium chloride buffer solutions with 10% of Tween-20 (MNT). Next, they were incubated for 1 hour with the blocking buffer followed by soaking for 4 hours with anti-DIG antibody (Roche Diagnostics) with a dilution of 1:2000, at room temperature. Several MNT washes were performed after and then the samples have been incubated with alkaline phosphatase (AP) buffer and stained with BM purple.

6.5 Reference and Notes

1. Pickering, S. U., Emulsions. *Journal of the Chemical Society, Transactions* **1907,** 91, 2001-2021.
2. Binks, B. P., Particles as surfactants - similarities and differences. *Current Opinion in Colloid & Interface Science* **2002,** 7, (1-2), 21-41.
3. Cauvin, S.; Colver, P. J.; Bon, S. A. F., Pickering stabilized miniemulsion polymerization: Preparation of clay armored latexes. *Macromolecules* **2005,** 38, (19), 7887-7889.
4. Melle, S.; Lask, M.; Fuller, G. G., Pickering emulsions with controllable stability. *Langmuir* **2005,** 21, (6), 2158-2162.
5. Velev, O. D.; Furusawa, K.; Nagayama, K., Assembly of latex particles by using emulsion droplets as templates .1. Microstructured hollow spheres. *Langmuir* **1996,** 12, (10), 2374-2384.
6. Dinsmore, A. D.; Hsu, M. F.; Nikolaides, M. G.; Marquez, M.; Bausch, A. R.; Weitz, D. A., Colloidosomes: Selectively permeable capsules composed of colloidal particles. *Science* **2002,** 298, (5595), 1006-1009.
7. Yow, H. N.; Routh, A. F., Release Profiles of Encapsulated Actives from Colloidosomes Sintered for Various Durations. *Langmuir* **2009,** 25, (1), 159-166.
8. Duan, H. W.; Wang, D. Y.; Sobal, N. S.; Giersig, M.; Kurth, D. G.; Mohwald, H., Magnetic colloidosomes derived from nanoparticle interfacial self-assembly. *Nano Letters* **2005,** 5, (5), 949-952.
9. Noble, P. F.; Cayre, O. J.; Alargova, R. G.; Velev, O. D.; Paunov, V. N., Fabrication of "hairy" colloidosomes with shells of polymeric microrods. *Journal of the American Chemical Society* **2004,** 126, (26), 8092-8093.
10. Chen, T.; Colver, P. J.; Bon, S. A. F., Organic-inorganic hybrid hollow spheres prepared from TiO2-stabilized pickering emulsion polymerization. *Advanced Materials* **2007,** 19, (17), 2286-2289.
11. Walsh, A.; Thompson, K. L.; Armes, S. P.; York, D. W., Polyamine-Functional Sterically Stabilized Latexes for Covalently Cross-Linkable Colloidosomes. *Langmuir* **2010**, 26, (23), 18039-18048.
12. Frelichowska, J.; Bolzinger, M. A.; Pelletier, J.; Valour, J. P.; Chevalier, Y., Topical delivery of lipophilic drugs from o/w Pickering emulsions. *International Journal of Pharmaceutics* **2009,** 371, (1-2), 56-63.
13. Prestidge, C. A.; Simovic, S., Nanoparticle encapsulation of emulsion droplets. *International Journal of Pharmaceutics* **2006,** 324, (1), 92-100.
14. Zhang, K.; Wu, W.; Guo, K.; Chen, J. F.; Zhang, P. Y., Synthesis of Temperature-Responsive Poly(N-isopropyl acrylamide)/Poly(methyl methacrylate)/Silica Hybrid Capsules from Inverse Pickering Emulsion Polymerization and Their Application in Controlled Drug Release. *Langmuir* **2009***,* 26, (11), 7971-7980.
15. Destribats, M.; Schmitt, V.; Backov, R., Thermostimulable Wax@SiO(2) Core-Shell Particles. *Langmuir* **2010***,* 26, (3), 1734-1742.
16. Kirchmeyer, M.; Koufany, M.; Sebillaud, S.; Netter, P.; Jouzeau, J. Y.; Bianchi, A., All-trans retinoic acid suppresses interleukin-6 expression in interleukin-1-stimulated synovial fibroblasts by inhibition of ERK(1/2) pathway independently of RAR activation. *Arthritis Research & Therapy* **2008,** 10, (6).
17. Firestein, G. S., Evolving concepts of rheumatoid arthritis. *Nature* **2003,** 423, (6937), 356-361.
18. Brinckerhoff, C. E.; Coffey, J. W.; Sullivan, A. C., Inflammation and collagenase production in rats with adjuvants arthritis reduced with 13-cis-retinoic acid. *Science* **1983,** 221, (4612), 756-758.
19. Nozaki, Y.; Yamagata, T.; Sugiyam, M.; Ikoma, S.; Kinoshita, K.; Funauchi, M., Anti-inflammatory effect of all-trans-retinoic acid in inflammatory arthritis. *Clinical Immunology* **2006,** 119, (3), 272-279.
20. Bryan, M.; Pulte, E. D.; Toomey, K. C.; Pliner, L.; Pavlick, A. C.; Saunders, T.; Wieder, R., A pilot phase II trial of all-trans retinoic acid (Vesanoid) and paclitaxel (Taxol) in patients with recurrent or metastatic breast cancer. *Investigational New Drugs* **2010**, 29, (6), 1482-1487.
21. Oh, S. W.; Moon, S. H.; Park, D. J.; Cho, B. Y.; Jung, K. C.; Lee, D. S.; Chung, J. K., Combined therapy with (131)I and retinoic acid in Korean patients with radioiodine-refractory papillary thyroid cancer. *European Journal of Nuclear Medicine and Molecular Imaging* **2011**, 38, (10), 1798-1805.
22. van der Hem, K. G.; Ossenkoppele, G. J., All-trans retinoic acid toxicity. *European Journal of Haematology* **1992,** 49, (3), 148-149.
23. Judith S, E., Zebrafish Make a Big Splash. *Cell* **1996,** 87, (6), 969-977.

24. Brittijn, S. A.; Duivesteijn, S. J.; Belmamoune, M.; Bertens, L. F. M.; Bitter, W.; De Bruijn, J. D.; Champagne, D. L.; Cuppen, E.; Flik, G.; Vandenbroucke-Grauls, C. M.; Janssen, R. A. J.; De Jong, I. M. L.; De Kloet, E. R.; Kros, A.; Meijer, A. H.; Metz, J. R.; Van der Sar, A. M.; Schaaf, M. J. M.; Schulte-Merker, S.; Spaink, H. P.; Tak, P. P.; Verbeek, F. J.; Vervoordeldonk, M. J.; Vonk, F. J.; Witte, F.; Yuan, H. P.; Richardson, M. K., Zebrafish development and regeneration: new tools for biomedical research. *International Journal of Developmental Biology* **2009,** 53, (5-6), 835-850.
25. Fako, V. E.; Furgeson, D. Y., Zebrafish as a correlative and predictive model for assessing biomaterial nanotoxicity. *Advanced Drug Delivery Reviews* **2009,** 61, (6), 478-486.
26. Akimenko, M. A.; Mari-Beffa, M.; Becerra, J.; Geraudie, J., Old questions, new tools, and some answers to the mystery of fin regeneration. *Developmental Dynamics* **2003,** 226, (2), 190-201.
27. Mari-Beffa, M.; Santamaria, J. A.; Murciano, C.; Santos-Ruiz, L.; Andrades, J. A.; Guerado, E.; Becerra, J., Zebrafish fins as a model system for skeletal human studies. *Thescientificworldjournal* **2007,** 7, 1114-1127.
28. Geraudie, J.; Monnot, M. J.; Ferretti, P., Caudal fin regeneration in wild-type and long-fin mutant zebrafish is affected by retinoic acid. *International Journal of Developmental Biology* **1995,** 39, (2), 373-381.
29. Shaw, D. A.; Keech, M., Effects of surfactants, metal-ions, and antiinflammatory drugs on release in vitro of acid-phosphatase from rat epidermal lysosomes. *Journal of Investigative Dermatology* **1975,** 64, (4), 285-285.
30. Trewyn, B. G.; Slowing, II; Giri, S.; Chen, H. T.; Lin, V. S. Y., Synthesis and functionalization of a mesoporous silica nanoparticle based on the sol-gel process and applications in controlled release. *Accounts of Chemical Research* **2007,** 40, (9), 846-853.
31. Stober, W.; Fink, A.; Bohn, E., Controlled growth of monodisperse silica spheres in micron size range. *Journal of Colloid and Interface Science* **1968,** 26, (1), 62-69.
32. Lu, J.; Choi, E.; Tamanoi, F.; Zink, J. I., Light-activated nanoimpeller-controlled drug release in cancer cells. *Small* **2008,** 4, (4), 421-426.
33. Bardine, N.; Donow, C.; Korte, B.; Durston, A. J.; Knochel, W.; Wacker, S. A., Two Hoxc6 Transcripts Are Differentially Expressed and Regulate Primary Neurogenesis in Xenopus laevis. *Developmental Dynamics* **2009,** 238, (3), 755-765.
34. Jansen, H. J.; Wacker, S. A.; Bardine, N.; Durston, A. J., The role of the Spemann organizer in anterior-posterior patterning of the trunk. *Mechanisms of Development* **2007,** 124, (9-10), 668-681.